

REMOTE SENSING OF THE ELECTRODYNAMIC
COUPLING BETWEEN THUNDERSTORM SYSTEMS
AND THE MESOSPHERE / LOWER IONOSPHERE

A DISSERTATION

SUBMITTED TO THE DEPARTMENT OF ELECTRICAL ENGINEERING

AND THE COMMITTEE ON GRADUATE STUDIES

OF STANFORD UNIVERSITY

IN PARTIAL FULFILLMENT OF THE REQUIREMENTS

FOR THE DEGREE OF

DOCTOR OF PHILOSOPHY

By

Steven Craig Reising

June 1998

© Copyright 1998 by Steven Craig Reising
All Rights Reserved

Dedication

In Memoriam

Flavian “Flip” Reising
(1912-1997)

M. Elizabeth “Betty” Reising
(1910-1988)

Joseph P. Bradley
(1895-1968)

J. Theresia Bradley
(1901-1981)

*For the love and labor of those who preceded us,
May we deserve their legacy.*

Abstract

In the past few years, dramatic experimental evidence has emerged, showing that tropospheric lightning discharges modify the mesosphere and the lower ionosphere through heating and ionization, producing gamma-ray bursts and optical emissions known as red sprites, blue jets, and elves. These transient electrodynamic coupling processes may have long-term effects such as chemical changes, persistent heating of ionospheric electrons, and increased production of mesospheric and stratospheric nitrogen oxides (NO_y). In order to assess the regional and global effects of the intense electrodynamic coupling of thunderstorms to the middle atmosphere, the occurrence rate of Sprites needs to be known over large areas of the Earth. Since continuous optical monitoring of Sprite occurrence on large spatial scales is not practical, a continuous proxy indicator for Sprite occurrence is needed.

Sprites are intense, transient luminous events in the mesosphere and lower ionosphere above thunderstorm systems. They extend from ~ 40 to ~ 90 km in altitude, are primarily red in color, and develop to full brightness in a few milliseconds. Sprites are nearly uniquely associated with positive cloud-to-ground lightning flashes, yet they occur in association with only a small subset of those flashes. The peak current of each flash, measured at high frequencies by the National Lightning Detection Network, is not a sufficient indicator of the likelihood of a positive cloud-to-ground lightning flash to produce a Sprite.

In this work, remote sensing of the electrodynamic coupling between thunderstorm systems and the mesosphere and lower ionosphere is accomplished by measurement of radio atmospherics in the ELF (extremely low frequency, here 15 Hz - 1.5 kHz) and VLF (very low frequency, here 1.5 - 22 kHz) ranges. Radio atmospherics (“sferics”) provide a unique signature of each lightning return stroke and propagate efficiently in the waveguide bounded by the Earth’s surface and the ionosphere. Novel digital signal processing techniques for ELF/VLF broadband measurements allow automated

detection and arrival azimuth determination of individual radio atmospherics. Arrival azimuth measurement is accomplished with $\pm 1^\circ$ precision for radio atmospherics propagating from Nebraska to Palmer Station, Antarctica, a source-to-receiver distance of $\sim 12,000$ km. Identification of the time of occurrence of sferics to ~ 1 -millisecond precision allows the identification of individual lightning discharges as the source of individual radio atmospherics. Broadband ELF/VLF measurements of radio atmospherics therefore allow the determination of characteristics of *those* lightning discharges which couple strongly to the middle atmosphere and lead to Sprite production.

Broadband measurements of sferics performed near Ft. Collins, Colorado, ~ 500 km from the causative lightning, demonstrate that the ELF sferic energy is a proxy indicator which can be used to estimate the number of Sprites produced by a thunderstorm with an accuracy of $\pm 25\%$. In addition, simultaneous video observations of Sprites reveal variable delays of up to 100 milliseconds between the positive cloud-to-ground flash and Sprite onset. Comparison with high-resolution photometer measurements demonstrate the simultaneity of Sprite luminosity and an ELF “second pulse,” radiated by electrical currents within the Sprite body [Cummer *et al.*, 1998]. Measurements of the second pulse are used to identify a quantitative relationship between the current in Sprites and total Sprite luminosity. Ultra-long range measurements at Palmer Station, Antarctica, show that Sprite-associated sferics have large ELF magnitudes in relation to non Sprite-associated sferics as measured at a range of $\sim 12,000$ km [Reising *et al.*, 1996]. These results suggest that a few appropriately placed ELF/VLF sferics receivers may be sufficient for estimation of global Sprite occurrence rates.

Acknowledgements

Near the middle of this work, I realized that the proverbial had become true; I was and am standing on the shoulders of giants. Our accomplishments would be impossible without the legacy of our predecessors and the guidance and collaboration of our contemporaries. The least I can do is to recognize some of the persons who have participated in this work and in my development as a scientist and as an engineer.

First and foremost, I would like to express my unequivocal gratitude to Professor Umran Inan, my principal advisor, for leading me into the field and the fray of scientific inquiry, for showing me by example how to succeed as a researcher and a scholar, and for supporting and promoting our efforts with seemingly boundless energy and dedication. Secondly, I would like to give wholehearted thanks to Dr. Tim Bell, my co-advisor, for his cheerful guidance in the development of a discerning eye and mind and for his ever-present wit and insight in facing our everyday challenges in the world of science. Professor Bob Helliwell passed along to me, as to so many, the original enthusiasm and inquisitiveness with which he founded the VLF Group more than forty years ago. Dr. Vikas Sonwalkar provided initial advice on the subject of sferics and continuing encouragement as his career took him to the University of Alaska Fairbanks. Professor Don Carpenter was a continual source of encouragement and support. I thank Professor Tony Fraser-Smith for his scientific discussions, for serving on my orals committee and for his first-rate sense of humor. I give special thanks to Professor J. W. Goodman for serving as my orals chairman and third reader of this dissertation.

The staff of the VLF Group made this work possible. Shao Lan Min and June Wang provided outstanding proposal support and cheerful advice. Bill Trabucco gave me unparalleled training on field work in the Arctic and Antarctic regions and on building reliable, fail-safe hardware. Jerry Yarbrough taught me time-saving and

essential techniques for broadband data analysis. Dr. Ev Paschal contributed indispensable engineering designs of the broadband receivers deployed both at Yucca Ridge and at Palmer Station.

Many graduates of the VLF Group contributed to my training. Dr. Dave Shafer introduced me to the fundamental skills of engineering design for reliability and gave me important advice on everything from negotiations with sponsors to travel in Chile. Dr. Bill Burgess provided data analysis software and many helpful hints on success as a Ph.D. student. Dr. Juan Rodriguez gave me guidance and encouragement during our three years as office mates. Darren Hakeman passed along excellent software for digital signal processing. Dr. Steve Cummer provided the 60 Hz removal algorithm and spheric viewing software. Finally, as both a student and a postdoctoral scholar, Dr. Victor Pasko provided many invaluable discussions on lightning and the electrodynamics of Sprites.

Current VLF Group students have contributed to this work. Chris Barrington-Leigh helped with analysis and interpretation of video and photometric data. Mike Johnson contributed Matlab algorithms and analysis ideas. Sean Lev-Tov and Dave Lauben expertly managed the computers, and Nikolai Lehtinen answered my incessant questions about Adobe Illustrator software. Several undergraduate students, principally Jason Deng and Ayse Inan, contributed countless hours of analysis of sferics waveforms.

Many from outside the STAR Laboratory played important roles in the development of this work. Professor Dave Sentman of the University of Alaska Fairbanks served as a mentor, guide and motivator through engaging scientific discussions in diverse places from Trapper Creek, Alaska, to Mont Saint-Michel, France. Dr. Martin Füllekrug, whom Tony Fraser-Smith recruited for postdoctoral work at Stanford, was outstanding in his encouragement, dedication and willingness to provide collaboration. Dr. James Weinman of NASA Goddard Space Flight Center provided continual enthusiasm for our subject and outstanding mentoring during my summer at Goddard and in the years which followed.

I would like to thank Dr. Walt Lyons and Tom Nelson of FMA Research, Inc., for hosting and assisting in our experiments at Yucca Ridge, Colorado, and for insights on Great Plains meteorology and “Sprite forecasts.” John Booth hosted my 1994 visit to Palmer Station, Antarctica, which proved to be one of the highlights of my graduate career. Since then, John Booth, Kevin Bliss and Glenn Grant have provided

talented and dedicated support for the Palmer Station experiments which provided much of the data for this dissertation.

In closing, I cannot forget the people that play the most pivotal role in all of our lives, our families. I am grateful to my parents, Flavian and Mary Jo, for teaching me the value of education, of committing myself to a goal and of persisting to achieve it. I thank my sister, Kathy, for her unflagging love and support. Finally, my wife Kathleen Zaleski has been the most patient and the most steadfast in her belief in my potential for success. For all of these giants in my life, I am forever grateful.

Steven C. Reising

*Stanford, California
May 31, 1998*

This research was made possible by the people of the United States through the sponsorship of the National Aeronautics and Space Administration (NASA) under grant NGT-30281 to Stanford University, a NASA Graduate Student Fellowship in Earth Systems Science. Data acquisition at Palmer Station, Antarctica, was sponsored by the National Science Foundation through grants OPP-9318596 and OPP-96115855 to Stanford University. Observations at Yucca Ridge Field Station, Colorado, were supported by the Air Force Research Laboratory under grant F19628-96-C-0075 and by the Office of Naval Research under AASERT grant N00014-95-1-1095.

Contents

Dedication	iv
Abstract	v
Acknowledgements	vii
1 Introduction	1
1.1 Sprites	2
1.2 Lightning Discharges and Thunderstorm Systems	4
1.2.1 Positive and Negative Discharges	4
1.2.2 Continuing Currents	5
1.2.3 Global Lightning	7
1.2.4 The National Lightning Detection Network	8
1.2.5 Mesoscale Convective Systems	9
1.3 Radio Atmospheric	12
1.4 Contributions of this Work	14
2 Broadband ELF/VLF Lightning Detection and Location	15
2.1 Broadband ELF/VLF Receiving Systems	16
2.1.1 ELF/VLF Receiver at Palmer Station, Antarctica	17
2.1.2 ELF/VLF Sferic Receiver at Yucca Ridge, Colorado	19
2.2 Sferic Detection	20
2.3 Sferic Arrival Azimuth Determination	23
2.4 Precision of Sferic Arrival Azimuth Determination	24
3 Association of Sprites and Cloud-to-Ground Lightning	30
3.1 Identification of Sprite Onset Time	30

3.2	Association of Sprites and Positive Cloud-to-Ground Flashes	32
3.3	Delays between Positive CG Flashes and Sprite Onsets	36
4	ELF Sferic Energy as a Proxy Indicator for Sprite Occurrence	39
4.1	Quantitative Analysis of VLF and ELF sferics	41
4.2	Medium Range Measurements at Yucca Ridge, Colorado	44
4.3	Ultra-Long Range Measurements at Palmer Station, Antarctica	47
4.3.1	Continuing Currents in Sprite-Associated Lightning Flashes	48
4.3.2	Sprite-Producing Storm on July 12, 1994	49
4.3.3	Sprite-Producing Storm on July 15, 1995	51
4.3.4	Application of ELF Proxy to Multiple Storms	52
4.4	ELF Radiation from Electrical Currents in Sprites	54
5	Summary and Suggestions for Future Work	65
5.1	Summary	65
5.2	Suggestions for Future Work	67
5.2.1	Assessment of the Global Distribution of Sprite Occurrence	67
5.2.2	ELF/VLF Proxy Indicator for the Occurrence of Elves	68
5.2.3	Multistation Measurements of Global Lightning Flash Rates	69
	Bibliography	72

List of Tables

2.1 Comparison of Palmer and Yucca Ridge broadband systems 19

List of Figures

1.1	Image of a Sprite recorded at ~ 550 km range on July 24, 1996.	2
1.2	Worldwide lightning flash density observations by the Optical Transient Detector orbiting at 750 km altitude and 70° inclination.	7
1.3	Bipolar structure of an Oklahoma winter thunderstorm.	10
1.4	Schematic of electrification of mesoscale convective systems, including positive CGs and horizontal discharges in the stratiform region.	11
2.1	ELF/VLF sferic data analysis block diagram.	16
2.2	ELF/VLF sferic receiver block diagram.	17
2.3	Palmer Station broadband ELF/VLF receiver frequency response.	18
2.4	Yucca Ridge broadband ELF/VLF sferic receiver frequency response.	20
2.5	Spectrogram of broadband data showing noise background, as measured at Palmer Station, Antarctica.	21
2.6	Map of great circle paths from North America to Palmer Station, Antarctica, a range of $\sim 12,000$ km.	25
2.7	Map of NLDN-detected positive CG lightning flashes in the western U.S. on August 1, 1996.	26
2.8	Magnitude and arrival direction spectrograms for VLF data recorded at Palmer Station, with simultaneous NLDN data.	27
2.9	Sferics histogram as function of both VLF peak intensity and arrival azimuth at Palmer Station on August 1, 1996.	28
2.10	Error histogram demonstrating arrival azimuth determination to $\pm 1^\circ$ at Palmer Station.	29
3.1	Determination of Sprite onset time from video observations.	31
3.2	NLDN lightning locations and camera field of view of western Kansas thunderstorm from Yucca Ridge, Colorado	34

3.3	Time delays between positive cloud-to-ground flashes and Sprite onsets.	37
4.1	Removal of power line interference from sferics data recorded at Yucca Ridge, Colorado.	42
4.2	Measurement of the VLF and ELF components of sferics recorded at Yucca Ridge, Colorado.	43
4.3	Histogram of the NLDN-recorded peak current for Sprite-associated and non Sprite-associated sferics on August 1, 1996.	45
4.4	Histogram of the ELF sferic energy for Sprite-associated and non Sprite-associated sferics on August 1, 1996.	46
4.5	Histogram showing the use of ELF sferic energy as a proxy indicator for Sprite occurrence.	47
4.6	Palmer Station sferics waveforms which have similar VLF peak intensity but widely differing ELF slow-tail magnitudes.	48
4.7	Maps of NLDN-recorded positive CG flash locations and Sprite-associated flashes on July 12, 1994, and July 15, 1995.	50
4.8	Histograms of NLDN peak current and ELF sferic energy in comparison with Sprite occurrence for July 12, 1994.	51
4.9	Histograms of NLDN peak current and ELF sferic energy in comparison with Sprite occurrence for July 15, 1995.	52
4.10	Histograms of NLDN peak current and ELF sferic energy for multiple storms in comparison with Sprite occurrence on August 1, 1996.	53
4.11	Infrared brightness temperature measured on the GOES 8 satellite on August 1, 1996.	55
4.12	Comparison of sferics waveforms with and without the second ELF pulse.	56
4.13	Simultaneous ELF second pulse and photometer measurements of Sprite luminosity at 08:24:00 UT on August 1, 1996.	57
4.14	Simultaneous ELF second pulse and photometer measurements of Sprite luminosity at 08:39:30 UT on August 1, 1996.	58
4.15	Linear relationship between Sprite charge moment and total Sprite luminosity for 17 Sprites on July 24, 1996.	59
4.16	Broadband sferics data measured at Yucca Ridge on July 24, 1996, showing ~56-ms delay between the first and second ELF pulses.	60

4.17	Simultaneous multi-anode photometer and broadband ELF data for the Sprite-associated sferic shown in Figure 4.16.	61
4.18	Broadband sferics data measured at Yucca Ridge on July 24, 1996, showing ~ 70 -ms delay between the first and second ELF pulses.	62
4.19	Simultaneous multi-anode photometer and broadband ELF data for the Sprite-associated sferic shown in Figure 4.18.	63
4.20	Relationship between continuing current charge moment and CG-to-Sprite delay for 17 Sprites on July 24, 1996.	64

Chapter 1

Introduction

Each lightning discharge dissipates a total energy of $\sim 10^9$ J, of which $\sim 10^6$ J is radiated as electromagnetic energy, during a duration of ~ 0.1 ms [Uman, 1987; pp. 322-323]. Energy released by a subset of lightning discharges couples to the mesosphere and the lower ionosphere, where the most dramatic visible effects are transient, luminous glows known as Sprites (see Figure 1.1), first recorded in 1989 [Franz *et al.*, 1990]. The characteristics of Sprites are described in Section 1.1. Each Sprite appears following a positive cloud-to-ground lightning discharge [Bocchippio *et al.*, 1995; Reising *et al.*, 1996]. The characteristics of lightning discharges and the thunderstorm systems relevant to Sprites are described in Section 1.2. The intensity of the lightning discharge, which is measured routinely by the National Lightning Detection Network, is not a sufficient indicator of whether or not a given positive discharge is likely to initiate a Sprite. In this work, lightning discharges are remotely characterized via the measurement of their electromagnetic signatures, known as radio atmospherics, which propagate efficiently in the Earth-ionosphere waveguide. Measurement of radio atmospherics allows detection of the properties of *those* lightning discharges which lead to Sprites and, consequently, of the total number of Sprites produced by a thunderstorm. The characteristics of radio atmospherics are described in Section 1.3.

1.1 Sprites

Sprites are transient luminous glows in the middle atmosphere above thunderstorms, arguably the most dramatic visible evidence of electrodynamic coupling between thunderstorm systems and the overlying mesosphere and lower ionosphere (see Figure 1.1). Sprites extend from ~ 40 to ~ 90 km in altitude and have transverse extents of ~ 10 to ~ 50 km [Sentman *et al.*, 1995; Lyons, 1996]. They develop to full brightness in 1-3 ms [Cummer *et al.*, 1998], but their luminosity may last for 10-100 ms [Fukunishi *et al.*, 1996; Winckler *et al.*, 1996; Lyons, 1996]. Low light level video observations of Sprites have been conducted from the Space Shuttle [Boeck *et al.*, 1995], from aircraft [Sentman and Wescott, 1993; Sentman *et al.*, 1995] and from the ground [Franz *et al.*, 1990; Lyons, 1994; 1996; Winckler *et al.*, 1996].

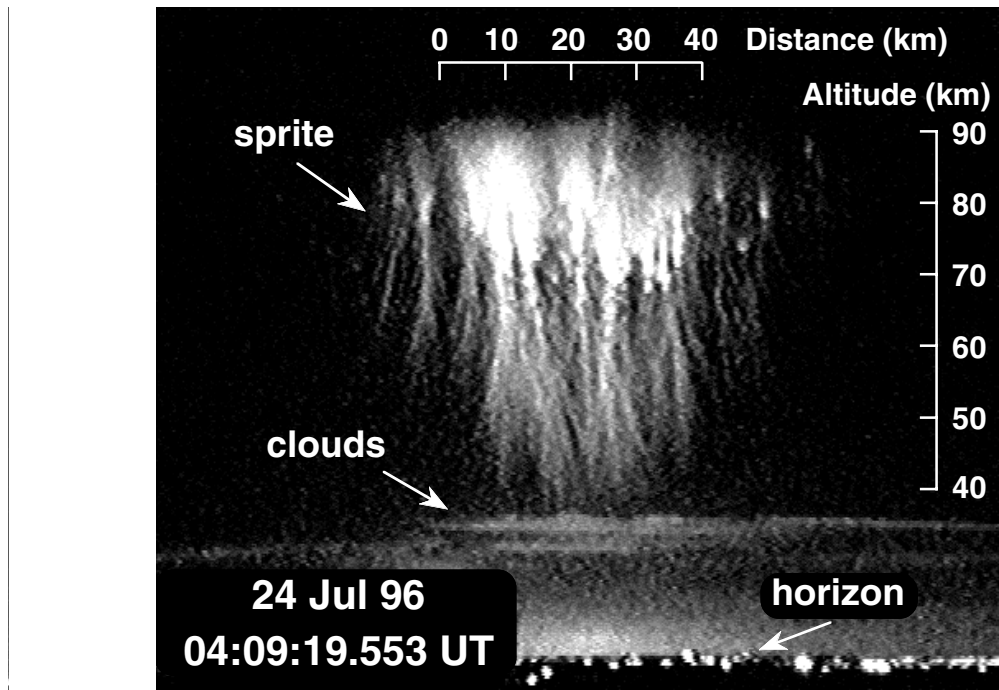


Figure 1.1: Image of a Sprite recorded by an intensified CCD video camera at Yucca Ridge, Colorado, at ~ 550 km range. Observations were made as a part of the Stanford University Fly's Eye Experiment.

Observations of other optical emissions provide additional evidence of electrodynamic coupling between thunderstorm systems and the middle atmosphere, including blue jets and blue starters from aircraft [Wescott *et al.*, 1995; 1996] and elves from the Space Shuttle [Boeck *et al.*, 1992] and from the ground [Fukunishi *et al.*, 1996; Inan

et al., 1997]. Other evidence of electrodynamic coupling includes VLF signatures of rapid changes in conductivity and ionization in the lower ionosphere [*Inan et al.*, 1988, 1993, 1995, 1996a; *Dowden et al.*, 1994] and radar detection of transient ionization patches above a thunderstorm [*Roussel-Dupré and Blanc*, 1997]. The observation of terrestrial gamma-ray flashes by the Burst and Transient Source Experiment is one of the most unexpected discoveries made by the Compton Gamma-Ray Observatory [*Fishman et al.*, 1994]. A number of satellite observations of gamma-ray flashes have been directly associated with individual sferics generated by positive CG discharges [*Inan et al.*, 1996b]. The gamma-ray photon energy extends above 1 MeV, indicating bremsstrahlung radiation from >1 MeV electrons, consistent with predictions of upward beams of runaway electrons accelerated by thundercloud electric fields [*Wilson*, 1925; *Bell et al.*, 1995; *Taranenko and Roussel-Dupré*, 1996; *Lehtinen et al.*, 1996; 1997].

Sprites are believed to be produced by intense quasi-electrostatic fields (tens of kV/m at ~ 70 km altitude) which exist at high altitudes following positive CG discharges [*Pasko et al.*, 1995, 1996, 1997; *Boccippio et al.*, 1995; *Winckler et al.*, 1996; *Fernsler and Rowland*, 1996]. These quasi-electrostatic fields lead to ambient electron heating (up to ~ 5 eV average energy), the ionization of neutrals and the excitation of optical emissions in the altitude range ~ 40 to ~ 90 km [*Pasko et al.*, 1997, and references therein]. The runaway electron mechanism may also play a role in Sprite generation [*Bell et al.*, 1995; *Taranenko and Roussel-Dupré*, 1996; *Lehtinen et al.*, 1996; 1997]. Another mechanism of interaction with the mesosphere and the lower ionosphere is the heating of ambient electrons by lightning electromagnetic pulses, which has been applied to explain the existence of elves [*Inan et al.*, 1991, 1996c; *Taranenko et al.*, 1993; *Rowland et al.*, 1995, 1996] and of Sprites [*Milikh et al.*, 1995].

For the quasi-electrostatic mechanism of Sprite production, the important parameters that determine whether or not a positive CG flash produces a Sprite are the altitude and magnitude of the thundercloud charge removed to ground. For a fixed altitude of removed charge, the single most important parameter in determining Sprite occurrence is the magnitude of the charge lowered to ground. The discharge duration plays a secondary role, as long as the charge removal time is shorter than the local relaxation time (ϵ_o/σ) at ~ 70 -90 km altitudes [*Boccippio et al.*, 1995; *Pasko et al.*, 1995; 1997].

1.2 Lightning Discharges and Thunderstorm Systems

In this dissertation we consider primarily cloud-to-ground (CG) lightning discharges, as opposed to intracloud discharges, which do not make electrical contact with the ground. This focus is appropriate because Sprites are nearly exclusively accompanied by CG flashes. In fact, the vast majority of prior research on lightning has also focused on CG discharges because of their potential for damage to property and living things, and because of their relative accessibility for study. It should be noted, however, that the number of intracloud discharges in a thunderstorm exceeds the number of CG discharges by a factor of $\sim 2-5$ [Uman, 1987; pp. 44-45], and that the energy released in intracloud discharges may play an important role in electrodynamic coupling to the middle and upper atmosphere.

1.2.1 Positive and Negative Discharges

The polarity of a CG lightning discharge is classified as “positive” or “negative” based on the polarity of its net effect on the charge of the thundercloud. If the net effect of the discharge is to move negative charge (electrons) from the cloud to the ground, it is called a *negative CG*. If it has the net effect of transferring positive charge from the cloud to the ground (electrons moving upward), then it is called a *positive CG*. This terminology is in common use in the lightning literature [Uman, 1987; pp. 9-10]. The total CG discharge is called a *flash* and has a typical duration of 0.1 - 1 s. A CG flash consists of a series of leaders, typically three or four, each followed by *return strokes*, which occur each time there is a completion of the electrical connection between the cloud’s charge reservoir and the ground. The first return stroke is initiated by the *stepped leader*, the visible channel following a high conductivity path formed by preliminary breakdown preceding the flash. If the flash ends when the first return stroke ceases, it is called a single-stroke flash. On the other hand, if additional charge is available in the cloud, a *dart leader* may propagate down the residual channel and initiate a subsequent return stroke. As many as 15 more return strokes may occur in the same flash, with typical delays between strokes of 30-100 ms [Uman, 1987; pp. 10-19].

Negative and positive CGs differ in their properties and occurrence rates. Positive

flashes are generally composed of a single stroke, sometimes followed by a period of continuing current (see Section 1.2.2). Positive CGs may dominate some winter storms, reportedly constituting up to 90-100% of the total lightning [Brook *et al.*, 1989]. However, overall lightning rates in winter are low, and summer thunderstorms produce predominantly negative CG flashes [Uman, 1987; p. 20]. Consequently, negatives represented >97% of the CG flashes in the continental U.S. during 1989-1991, as recorded by the National Lightning Detection Network (see Section 1.2.4) [Orville, 1994]. An increase in the fraction of positive lightning in summer thunderstorms is correlated with increasing latitude and with increasing elevation above sea level [Uman, 1987; p. 20].

One of the most complete descriptions of return stroke currents is based on measurements of discharges to towers in Switzerland (e.g., [Berger *et al.*, 1975]). The currents were derived from measurements of the voltages induced in resistive shunts located on two towers reaching 55 m above the summit of Mt. San Salvatore [Uman, 1987; p. 120]. Based on these measurements, the average duration of negative first return strokes is ~ 0.1 ms. The duration of positive first return strokes has more variability, with an average value of 0.2-0.6 ms [Berger *et al.*, 1975]. However, their recorded waveforms may have been altered by the electrical characteristics of the tower and measuring circuit and by the difference between discharges to tall objects and discharges to ground [Uman, 1987; p. 121]. Peak current magnitudes measured by Berger *et al.* [1975] were observed to fit a log-normal distribution. Negative first return strokes had a median peak current of 20-40 kA, with levels of 200 kA reached only 1% of the time. Subsequent return strokes carried approximately half the peak current of first strokes. Positive return strokes exhibited the same median peak current as first return strokes, but in extreme cases were much larger, with 5% of the positive peak currents exceeding 250 kA [Uman, 1987; pp. 122-125].

1.2.2 Continuing Currents

The total charge lowered from a thundercloud at a given altitude to the ground in a lightning discharge is believed to be the most important parameter in determining its potential for producing a Sprite (see Section 1.1 and [Pasko *et al.*, 1997]). The charge lowered to ground can be computed by integrating the current waveform over time. Typical values of charge transfer in the < 0.1 ms duration of a negative return stroke

are $\sim 3\text{-}5$ C for first strokes and ~ 1 C for subsequent strokes [Uman, 1987; p. 125]. For positive return strokes, Berger *et al.* [1975] found that the median was ~ 15 C, but that 5% of positive return strokes transferred more than 150 C to ground. Since peak currents rarely exceed 300 kA [Brook *et al.*, 1982], the charge transfer in a return stroke of ~ 0.5 ms maximum duration is expected to be < 120 C, assuming a simple approximation of a half-cycle of a sine wave for the time-dependence of current in the return stroke. *Continuing currents* are required for larger cloud-to-ground charge transfers. In these cases, current continues to flow in the cloud-to-ground channel for one to hundreds of milliseconds following the return stroke [Uman, 1987; pp. 13-14, 172]. Long-lasting continuing currents are of economic interest because they are responsible for the most serious heating damage due to lightning, including many electrical and forest fires [Rakov and Uman, 1990].

Brook *et al.* [1982] documented continuing currents associated with positive CGs from winter thunderstorms on the Hokuriku coast in Japan. They recorded field-change measurements for 12 positive CGs, ten of which were followed by continuing current. The two strongest continuing currents were sustained at a remarkably high level of 10-100 kA for several milliseconds, transferring a total charge to ground of ~ 300 C in 4 ms and of ~ 200 C in 10 ms. The current magnitude was observed to vary on a 1-ms time scale. A more recent study of winter thunderstorms in the same area of Japan measured > 30 positive CGs. The three largest positive CGs were accompanied by continuing currents transferring 200-400 C of charge [Goto and Narita, 1995]. Based on observations of five summertime severe storms, Rust *et al.* [1981] reported continuing current durations of 30-240 ms in 31 positive CG flashes. Brook *et al.* [1982] observed continuing currents in association with negative CGs, but the magnitudes of continuing currents were an order of magnitude lower than those associated with positive CGs. Other measurements confirm that strong continuing currents are typically associated with positive CGs [Uman, 1987; p. 201].

In summary, removal of large amounts of charge, > 120 C, in a single CG return stroke lasting < 0.5 ms requires peak currents of > 300 kA, a level which is rarely if ever reached. Continuing current of > 1 ms duration after the first return stroke of the flash is required to transfer larger amounts of charge from cloud to ground.

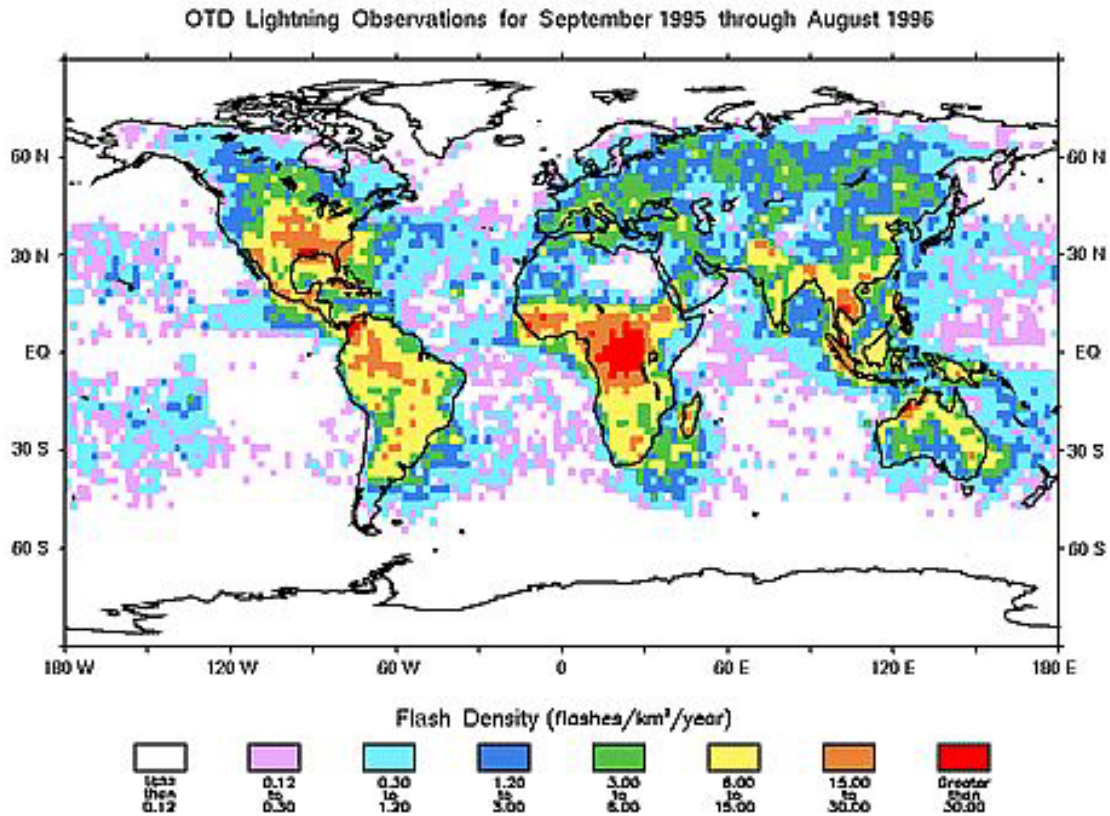


Figure 1.2: Worldwide flash density observations for a one-year period, measured by the Optical Transient Detector orbiting at 750 km altitude and 70° inclination. Courtesy of Dr. H. J. Christian. Available on the World Wide Web at <http://thunder.msfc.nasa.gov/otd.html>.

1.2.3 Global Lightning

The often-quoted global lightning occurrence rate of ~ 100 flashes per second was reported in 1925, based on the product of the typical lightning rate for thunderstorms in England (200 flashes per hour), and the average number of thunderstorms on the globe (1800), which was derived from land and maritime records of the number of days per year during which thunder is heard [Brooks, 1925]. The first measurements of lightning from space were in general agreement with the rate of ~ 100 flashes per second, based on an equivalent of five minutes of global lightning data measured at local midnight [Orville and Henderson, 1986]. A sufficient sample of global lightning data was not available to test the ~ 100 flashes per second hypothesis until the launch of the Optical Transient Detector in April 1995 into a 750-km altitude, 70° inclination orbit. The Optical Transient Detector measurements indicate a rate of ~ 40 flashes

per second worldwide, globally distributed as shown in Figure 1.2 [Christian *et al.*, 1996]. Lightning is preferentially produced over land because of the strong updrafts in continental clouds as opposed to oceanic clouds [Goodman and Christian, 1993].

1.2.4 The National Lightning Detection Network

The National Lightning Detection Network (NLDN) has provided real-time lightning data (within 40 seconds) covering the continental United States since 1989 [Cummins *et al.*, 1998]. The NLDN was created by merging regional networks covering the Western U.S. [Krider *et al.*, 1980] and the Midwest [Mach *et al.*, 1986] with the East Coast network operated by the State University of New York at Albany (SUNYA Network) [Orville *et al.*, 1983]. The sensors used in this network were gated, wideband magnetic direction finders manufactured by Lightning Location and Protection, Inc., and were designed to measure only CG lightning flashes [Krider *et al.*, 1976; 1980]. During the same period, a network based on time-of-arrival sensors manufactured by Atmospheric Research Systems, Inc., was installed nationwide [Lyons *et al.*, 1989]. During 1992, Lightning Location and Protection, Inc., developed the Improved Accuracy from Combined Technology method for locating lightning by combining information from both magnetic direction finders and time-of-arrival sensors. This allowed the NLDN to upgrade existing sensors of both types and to combine them with new sensors in order to form a new 106-station upgraded NLDN network, which was completed in 1995 [Cummins *et al.*, 1998].

The NLDN currently provides information on the time, location, intensity, number of strokes per flash and the location accuracy of each flash. The NLDN data used in this work is “flash data,” i.e., the data contain timing, location and intensity information about only the first return stroke of each CG flash. The NLDN timing information is accurate to universal coordinated time to within 1 ms. The median accuracy of the CG location is 0.5 km, verified by triangulated video observations [Idone *et al.*, 1998a].

The single measure of return stroke intensity provided by NLDN is the return stroke peak current. The peak current measurement contains no information about the duration of the return stroke nor about continuing currents. Since the rise time of return strokes is $\sim 5 \mu\text{s}$ for negative strokes and $\sim 20 \mu\text{s}$ for positive strokes, this measurement contains an effective highpass filter at or above $\sim 50 \text{ kHz}$. However, in

positive CGs with continuing currents, the majority of the cloud-to-ground charge transfer occurs during the continuing current of >1 ms duration (see Section 1.2.2). Therefore the NLDN peak current measurement does not provide a reliable estimate of the total cloud-to-ground charge transfer. The peak current data are provided by NLDN in terms of the normalized magnetic signal strength (M_{peak}). In this work, we obtain the peak current (I_{peak}) from the M_{peak} by using the most recent calibration published prior to 1998, given by Equation 5 of *Idone et al.* [1993]:

$$I_{\text{peak}}(\text{kA}) = 4.20 + 0.171 \times M_{\text{peak}}$$

Additionally, the NLDN data contain the polarity of the first return stroke of the lightning flash. *Brook et al.* [1989] confirmed correct polarity determination of the SUNYA lightning detection network, one of the predecessors of the NLDN, based on electric field change studies of lightning from winter storms in New York state. The authors emphasized the limitation that at >600 km range between the lightning and a magnetic direction finding sensor, the inverted “skywave” reflected from the ionosphere is often much stronger than the direct “ground wave,” sometimes resulting in polarity misidentification. In most situations, though, multiple NLDN sensors are located within ~ 600 km from the source lightning.

In this work, the term “CG flash” is used when the literal meaning is “first return stroke of the CG flash.” “Positive CG” or “negative CG” implicitly refer to the first return stroke of the flash.

1.2.5 Mesoscale Convective Systems

Mesoscale convective systems are intermediate-sized meteorological systems which are larger than individual cumulonimbus cells but smaller and shorter-lived than synoptic disturbances [*Barry and Chorley*, 1987; p. 203]. The mesoscale convective systems referred to in this work are midlatitude and subtropical systems which consist of nearly circular clusters of many interacting thunderstorm cells. They are not associated with weather fronts and usually develop during weak synoptic-scale flow. Mesoscale convective systems span transverse scales of $>10,000$ km² and have lifetimes of 6-24 hours. When a mesoscale convective system exceeds a horizontal extent of 100,000 km², it is classified as a mesoscale convective complex. These complexes

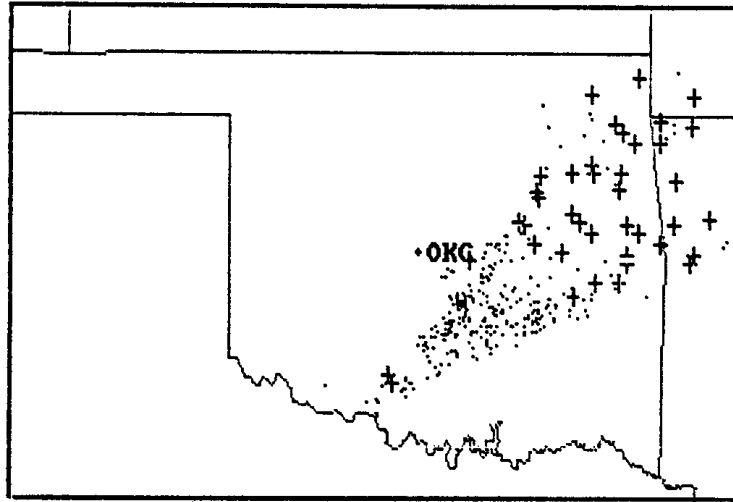


Figure 1.3: From *Brook et al.* [1989]. Winter thunderstorm of January 17, 1988. The storm started at the Oklahoma-Texas border and continued as it moved northeast for a period of 14 hours. The negative (dots) and positive (crosses) CG return strokes are separated into two distinct regions.

are common over the Great Plains and the midwestern U.S. during the spring and summer where they account for perhaps 80% of growing season rainfall [*Barry and Chorley*, 1987; pp. 203-207; *Moran and Morgan*, 1997; pp. 311-313].

Orville et al. [1988] first reported a “bipolar” pattern in the geographical distribution of positive and negative CGs in many mesoscale convective systems. They found that CG locations were “polarized” into two regions, one predominantly composed of positive CGs and the other of negative CGs, separated by 60-200 km (see Figure 1.3). The direction between the two “bipoles” is that of the upper level (geostrophic) wind, with the positive CGs occurring on the downwind side of the storm. The bipolar pattern was observed in all seasons, with the clearest defined separation of the polarities occurring in winter [*Orville et al.*, 1988]. *Rutledge et al.* [1990] found that negative CGs are concentrated in the convective core of the storm, where the updrafts and rain rates are strongest, and that positive CGs are predominant in the stratiform region. The classical model of thunderstorm electrification, with an area of distributed positive charge overlying an area of negative charge, explains the dominance of negative CGs in the convective core (see top left of Figure 1.4). *Rutledge et al.* [1990] modeled the stratiform region electrification as an inverted dipole, with positive charge on the bottom and negative charge on top (see top right of Figure 1.4), as a result of *in-situ* charging processes independent of those in the convective core.

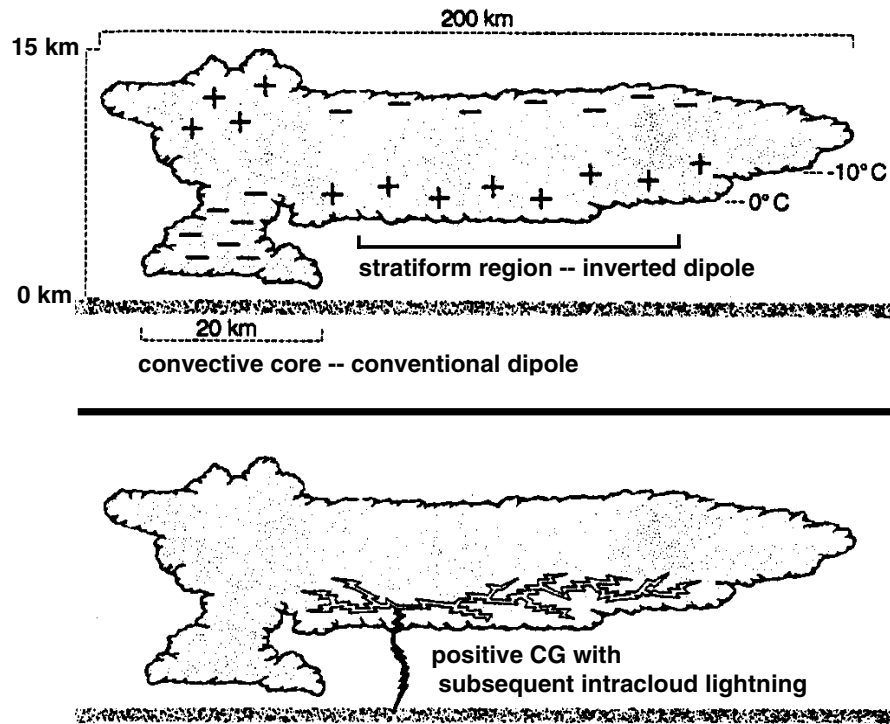


Figure 1.4: Adapted from *Lyons* [1996]. (Top) Schematic of the typical Great Plains mesoscale convective system associated with Sprites. Models of electrification are shown for the convective core on the left and stratiform region on the right. (Bottom) Positive CG causes charge rearrangement in the cloud, which may induce subsequent intracloud “spider” discharges in the stratiform region.

Related work indicates that in the convective core, extensive vertical growth of the thundercloud leads to the creation of a mixed-phase layer between 0°C and -40°C , where graupel particles (1-10 mm snowballs) form and contribute significantly to the charging of the thundercloud [Williams, 1995; pp. 36-38]. These “deep convective regions” may be necessary for the formation of downwind horizontally extensive stratiform regions, where the highest percentage of positive CGs occur [Rutledge *et al.*, 1993]. Electric field soundings aboard balloons indicate that the stratiform regions of mesoscale convective systems have multiple vertical layers of space charge, which are nearly uniform in the horizontal dimension and each hold up to ~ 1000 C of charge [Stolzenburg *et al.*, 1994; Marshall *et al.*, 1996]. In light of observations of large continuing currents associated with positive CGs (see Section 1.2.2), this charge structure indicates that large reservoirs of positive charge exist in the horizontally extensive (>100 km) stratiform regions of mesoscale convective systems. In some cases, a positive CG and continuing currents may drain charge from only part of the reservoir,

and the resulting charge rearrangement in the stratiform region may induce subsequent intracloud discharges, known as “spider” lightning [Williams, 1995; pp. 50-52; Lyons, 1996] (see also Section 3.3). Sprites are associated with the occurrence of positive CGs, and most Sprites have been observed overlying the stratiform regions of mesoscale convective systems in the mature or decaying phases (e.g., [Lyons, 1996]). The predictions of quasi-electrostatic models of Sprite production (see Section 1.1) are consistent with the hypothesis that large reservoirs of positive charge exist in the stratiform regions of mesoscale convective systems.

1.3 Radio Atmospheric

In this dissertation, broadband ELF/VLF measurements of radio atmospheric are used to assess the characteristics of individual lightning discharges from distances of up to $\sim 12,000$ km. Lightning radiates electromagnetic energy from a few Hz [Fukunishi et al., 1997] up to many tens of MHz [Weidman and Krider, 1986]. Consistent with the time and spatial scales of lightning discharges, the peak power radiated by a lightning discharge is in the ELF (extremely low frequency, here 15 Hz - 1.5 kHz) and VLF (very low frequency, here 1.5 kHz - 22 kHz) ranges [Uman, 1987; p. 118]. Radio atmospheric are the electromagnetic signals in the ELF/VLF frequency ranges that are launched into the Earth-ionosphere waveguide by lightning discharges [Budden, 1961; pp. 5,69]. Radio atmospheric are commonly called “sferics,” where the modified spelling is used to avoid confusion with terms such as “spherical geometry.” Sferics propagate with low but variable attenuation, typically $\sim 2-3$ dB/1,000 km, depending upon day/night, land/ocean and east/west propagation conditions, and can therefore be observed at large distances ($>12,000$ km) from the source [Davies, 1990; pp. 367, 387-389]. The parallel-plate waveguide which guides the propagation of sferics has as its boundaries the ground and the lower boundary of the D-region of the ionosphere, which at VLF frequencies is ~ 70 km altitude during the day and $\sim 80-85$ km altitude at night [Thomson, 1993; Cummer, 1997].

Radio wave propagation at these frequencies is typically analyzed in terms of waveguide modes, characterized as quasi-transverse electric and quasi-transverse magnetic modes in the VLF frequency range [Budden, 1962]. All of the modes except one have cutoff frequencies at integer multiples of ~ 1.8 kHz, the frequency with a free-space wavelength equal to the twice the height of the Earth-ionosphere waveguide,

~ 80 - 85 km at night [Cummer, 1997]. The single mode which has no cutoff frequency and which propagates in the Earth-ionosphere waveguide at frequencies below ~ 1.8 kHz is the quasi-transverse electromagnetic mode. Models of the quasi-transverse electromagnetic mode of propagation have been used previously to obtain estimates of the current moment of the source lightning, and to infer the magnitude of the charge lowered from the cloud to ground [Bell *et al.*, 1996, 1998; Cummer and Inan, 1997]. The quasi-transverse electromagnetic mode does not overlap the VLF frequency range because its attenuation increases exponentially with frequency, and most quasi-transverse electromagnetic signals are strongly attenuated above ~ 1 kHz [Greifinger and Greifinger, 1986; Sukhorukov and Stubbe, 1997].

At long ranges (e.g., 5,000-12,000 km), sferics are repeatedly observed to have an oscillating VLF portion lasting ~ 1 ms, sometimes followed by an ELF “slow tail” (e.g., [Hepburn, 1957; Taylor and Sao, 1970; Sukhorukov, 1992; Sukhorukov and Stubbe, 1997]). The term “slow tail” denotes its late arrival; the first maximum of the ELF slow tail is delayed in time with respect to the VLF onset by an amount related to the propagation distance [Wait, 1960; Sukhorukov, 1992]. This delay is a simple result of the difference in phase velocities; the ELF slow tail propagates in the quasi-transverse electromagnetic mode with a phase velocity of $\sim 0.9 c$, while the VLF portion propagates in the quasi-transverse electric and quasi-transverse magnetic modes with a phase velocity much closer to c , the speed of light [Sukhorukov and Stubbe, 1997; Cummer, 1997]. Theoretical calculations show that the ELF slow tail is excited at significant levels only by source lightning discharges with a continuing-current component with significant variations on the time scale of ~ 1 - 3 ms [Wait, 1960]. In this dissertation, we make use of this fact to deduce the strength of continuing currents with duration ~ 1 - 3 ms based on remote measurements of the ELF slow tails of sferics at large source-to-receiver distances ($\sim 12,000$ km).

1.4 Contributions of this Work

The contributions of this dissertation are as follows:

- Developed novel digital signal processing techniques for automated detection and arrival azimuth determination of radio atmospherics (“sferics”) in broadband ELF/VLF data on a continuous basis. Determination of the arrival azimuth of sferics is based on the VLF Fourier Goniometry technique [Burgess, 1993]. We demonstrated arrival azimuth measurement with $\pm 1^\circ$ precision for sferics propagating from Nebraska to Palmer Station, Antarctica, a source-to-receiver distance of $\sim 12,000$ km.
- Based on ELF measurements of sferics at Palmer Station, Antarctica, demonstrated the first evidence of continuing currents in Sprite-producing positive CG lightning flashes. The continuing currents flow from cloud to ground for $\sim 1-3$ ms following the positive return stroke. The radiation from these currents enhances the ELF slow tails of sferics, which are observed at $\sim 12,000$ km from their source lightning.
- Based on ELF measurements of sferics at Yucca Ridge, Colorado, developed a proxy indicator for Sprite occurrence which can estimate the number of Sprites produced above a mesoscale convective system.
- Through measurements of ELF energy radiated from Sprites themselves, identified a quantitative relationship between the current in Sprites and total Sprite luminosity.